

SPIN GLASS FREEZING AND SUPERCONDUCTIVITY IN $\text{YBa}_2(\text{Cu}_{1-x}\text{Fe}_x)_3\text{O}_7$ ALLOYS

I. Mirebeau, M. Hennion - *Laboratoire Léon Brillouin (CEA-CNRS)*
CEN-Saclay, 91191 Gif-sur-Yvette Cedex, France

J. Dianoux, *Institut Laue Langevin*
156X Centre de Tri, 38042 Grenoble Cedex, France

V. Caignaert, *Laboratoire CRISMAT I.S.M.*,
Université de Caen, 14032 Caen, France

T.E. Phillips, K. Moorjani, *Applied Physics Laboratory,*
The John Hopkins University, Laurel, Maryland 20707, USA

We have studied the dynamics of the iron spins in superconducting $\text{YBa}_2(\text{Cu}_{0.94}\text{Fe}_{0.06})_3\text{O}_7$ by neutron time-of-flight measurements. Two samples were investigated with slightly different characteristics, as shown by resistivity and neutron diffraction measurements. The same dynamical anomalies are observed by neutrons in both samples. Differences appear qualitative but not quantitative. In the whole temperature range, the q-dependence of the magnetic intensity mainly reflects the magnetic form factor of iron which shows that the iron spins are almost uncorrelated. The elastic and quasielastic intensities strongly vary with temperature. A spin glass like freezing is revealed at low temperature by a sharp decrease of the quasielastic intensity, an increase of the "elastic" or resolution limited intensity and a minimum in the quasielastic width. The freezing temperature ($T_f = 18$ K) corresponds to that already determined by a magnetic splitting in Mössbauer experiments. Above T_f , the relaxation of the iron spins in the paramagnetic state is modified by the occurrence of superconductivity. We observe an increase of the quasielastic intensity and of the quasielastic width at the superconducting transition.

In the superconducting ceramics $\text{YBa}_2(\text{Cu}_{1-x}\text{Fe}_x)_3\text{O}_7$ the substitution of iron for copper leads to a rather slow decrease of the superconducting temperature T_c ¹. Electron microscopy², neutron diffraction² and Mössbauer experiments³ show that the Fe atoms mainly substitute on the Cu_1 sites in agreement with energy considerations for the thermal equilibrium state. Moreover, Mössbauer experiments show the occurrence of a Zeeman splitting in the spectra, indicating a freezing process of the Fe spins below some temperature T_f (fig.1). Interestingly enough, the spin freezing does not suppress the superconductivity. The nature of the correlations between the Fe atoms below T_f (ferromagnetic, antiferromagnetic or uncorrelated) has been controversial due to the strong difficulties in analysing the Mössbauer spectra. Therefore, this system provides a very interesting opportunity to investigate the interplay between magnetism and superconductivity by neutron scattering measurements.

We have performed inelastic neutron scattering measurements in order to study (i) the relaxation of the iron spin-above T_f (is it modified by the occurrence of the superconducting state ?) (ii) the characteristics of the

freezing itself, with a typical time window ($\sim 10^{-11}$ s) comparable to that of the Mössbauer probe. The concentration $x = 0.06$ is particularly suitable for this study since T_c and T_f are rather far from each other ($T_c \sim 65$ to 80 K, see Fig.1), $T_f \sim 18$ K. The time of flight measurements, performed with an excellent resolution, yield new and original informations. At low temperature, a spin-glass like freezing is clearly evidenced, which has all the characteristics previously observed in usual metallic spin glasses. At higher temperature, the enhancement of the quasielastic intensity and of the quasielastic width which occurs near the superconducting transition strongly suggests a coupling between the iron and the copper spin dynamics. These experiments extend those previously reported⁴ where only the spin glass freezing was clearly apparent. A short report of the present ones has been given in reference 5.

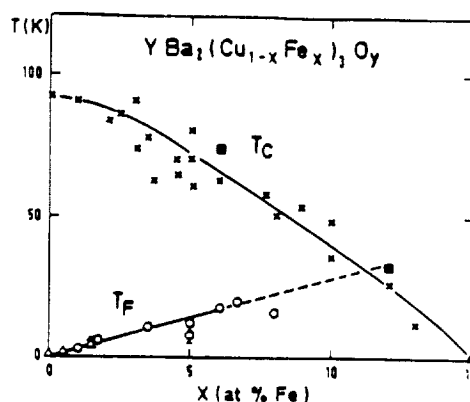


Fig.1. Typical superconducting temperatures $T_c(x)$ and freezing temperatures T_f in the $\text{YBa}_2(\text{Cu}_{1-x}\text{Fe}_x)_3\text{O}_y$ as measured from various authors^{1,3}. T_f is determined from Mössbauer (o) or NQR (Δ) measurements. (■) T_c values of our own samples.

1. SAMPLE PREPARATION AND CHARACTERIZATION

We compare here two samples of the same nominal concentration but with slightly different characteristics. These two samples of $\text{YBa}_2(\text{Cu}_{1-x}\text{Fe}_x)_3\text{O}_y$ with $x = 0.06$, $y \sim 7$, called samples a and b, were prepared respectively at B. Raveau Laboratory (Caen, France) and at Johns Hopkins Applied Phys. Lab. (Laurel, MD, USA). The procedure of preparation was basically the same in both cases. Appropriate amounts of Y_2O_3 , BaCO_3 , CuO and Fe_2O_3 in fine mesh powders were ground, pressed and heated at 950°C for 50 hours and then cooled over 15 hours in a constant O_2 flux. This procedure was repeated several times. After the final firing the samples were stored in a dry atmosphere. The samples used for neutron measurements were shaped in cylinders of 12mm diameter and 5cm length.

As shown in Fig.2, the neutron diffraction patterns correspond to a mean tetragonal phase, but small orthorhombic domains might be present as shown previously by electron microscopy². The lattice constants, determined from the peak positions by a Rietveld refinement are the same in the two samples. Small differences in the peak intensities can be related either to slightly different occupancies at the oxygen and Fe sites or to preferential grain orientations. In sample a, all the observable Bragg peaks belong to the structure whereas in sample b small peaks of impurities (BaCuO_2 mainly) are clearly visible between the main Bragg peaks.

Resistivity measurement (Fig.3) shows for sample a an onset of the superconducting transition at $T_c = 78$ K. In sample b, the resistivity clearly shows a slight maximum versus temperature, then a decrease below 63 K. This maximum in the resistivity curve is enhanced in the more concentrated samples and suggests that this second sample is rather close to a semiconducting behavior. Most probably, in sample a, all the Fe atoms occupy the Cu^{I} sites (Cu-O chains) while in sample b, a small fraction of iron might occupy the Cu^{II}

sites (Cu-O planes) which are mainly responsible for superconductivity. We note that some substitution of Fe on the planar sites has been already achieved^{2,6}, depending on the heat treatment, but seems to be rather difficult to obtain. Extended neutron and X-rays measurements on our two samples are being performed in order to clear this point.

Magnetization measurements indicated a diamagnetic volume of about 36% at low temperature and a superconducting transition in rather good agreement with the previous determinations ($T_c \sim 74$ K in sample a).

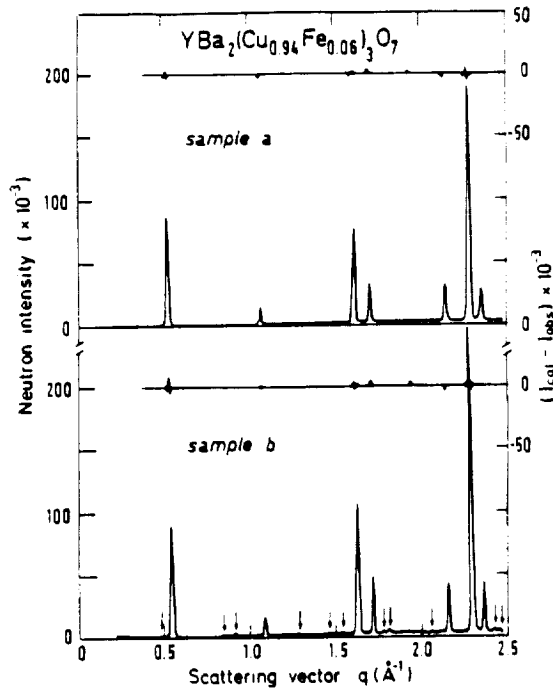


Fig.2. Neutron diffraction patterns in the two $\text{YBa}_2(\text{Cu}_{0.94}\text{Fe}_{0.06})_3\text{O}_7$ samples at 300 K. In 2b the arrows indicate impurity peaks (of BaCuO_2 mainly). Rietveld refinements are also plotted.

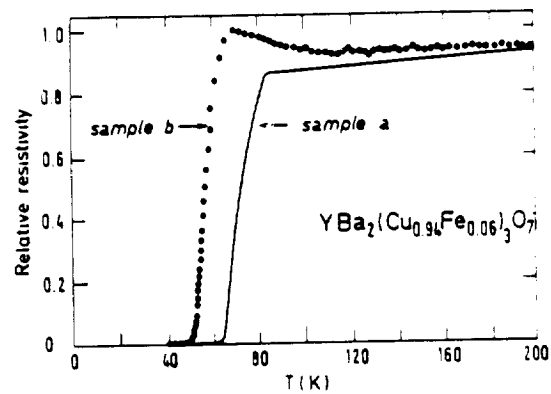


Fig.3. Relative resistance as a function of temperature in the two $x=0.06$ samples.

2. TIME OF FLIGHT NEUTRON MEASUREMENTS

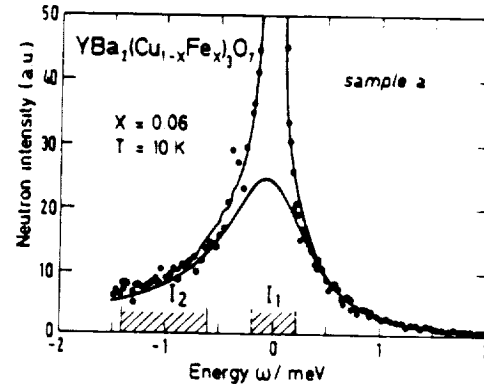
The Time of Flight (TOF) neutron scattering measurements were performed on the spectrometer IN6 of the high neutron flux source of ILL (Grenoble). In these experiments a monokinetic neutron pulse, corresponding to an incident neutron wavelength λ of 5 Å was selected by a "chopper" disk. The neutrons scattered by the sample were registered as a function of their time of arrival in each of the 336 counters which were positioned at selected angles θ between the Bragg peak positions. The range of the scattering vector q ($q = \frac{4\pi \sin \theta}{\lambda}$ where

2θ is the scattering angle) was $0.1 < q < 2.1 \text{ Å}^{-1}$, a range which roughly corresponds to the one covered in the diffraction patterns of Fig.2. Due to the high neutron flux source and to the use of a triple graphite monochromator, very good statistics could be achieved with a rather short counting time of about 4 hours at each temperature. The energy resolution of the spectrometer of 80 μeV corresponds to a typical time window of 10^{-11} s. The temperature was varied from 300 K to 1.8 K using a helium cryostat.

In a typical TOF spectrum, measured for a given value of the scattering angle 2θ , the neutron intensity is plotted as a function of time, or equivalently as a function of the energy transfer ω between the neutrons and the sample.

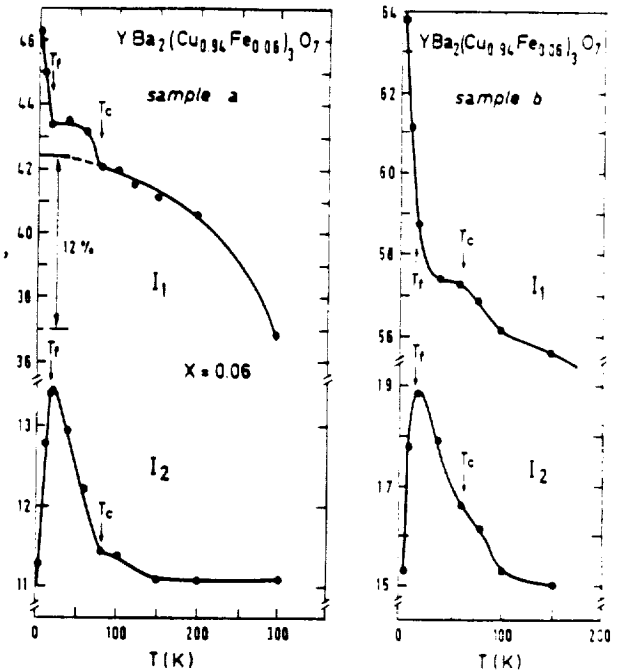
In pure $\text{YBa}_2\text{Cu}_3\text{O}_7$, a TOF spectrum consists of an elastic signal of nuclear origin and of an inelastic one due to the phonons. When the temperature decreases, the elastic intensity slightly increases due to the Debye Waller effects, whereas the phonon contribution decreases. In the substituted samples, the elastic intensity may have also a magnetic contribution and we observe in addition a quasielastic signal due to the relaxation of the iron spins. Focusing on the quasielastic region, we report in Fig.4 a typical TOF spectrum for the $x = 0.06$ sample as measured at the temperature of 10 K for a q value of 0.7 \AA^{-1} .

Fig.4. Typical time of flight spectrum measured at 10 K for a q -value of 0.7 \AA^{-1} in the sample a. The domain of energy integration corresponding to the intensities I_1 and I_2 (see text) are shown by dashed areas. The solid lines are fits to the data according to equation (1)



In fig.5a, we have plotted the temperature dependence of the intensities I_1 and I_2 , measured at $q = 0.7 \text{ \AA}^{-1}$ and corrected for background. I_1 corresponds to an integration of the TOF spectrum within the elastic window, in the energy range $(-0.2, 0.2) \text{ meV}$, and possesses an elastic and a quasielastic contribution. I_2 is the intensity integrated just aside the elastic signal, in a purely inelastic energy range $(-1.4, -0.6) \text{ meV}$ where the phonon contribution is small. We notice that both I_1 and I_2 present anomalies at the freezing and at the superconducting transitions. A very similar behavior is observed for the other sample b (Fig.5b). However, in the second sample which is clearly less homogeneous, as shown by the neutron diffraction and resistivity measurements, we note that although the freezing transition is still very well defined, the anomalies which occurred in the T_c region are much more smeared.

Fig.5. Intensities I_1 and I_2 versus temperature measured at $q \sim 0.7 \text{ \AA}^{-1}$ for the two samples a and b. The solid lines are a guide to the eye.



The corrected spectra were fitted by the sum of a delta function of norm $c_1(q)$ and of a quasielastic scattering function $S(q,\omega)$ convoluted with experimental resolution. Assuming a lorentzian shape for the relaxation process, and a Bose statistics for the magnetic excitations, it may be written :

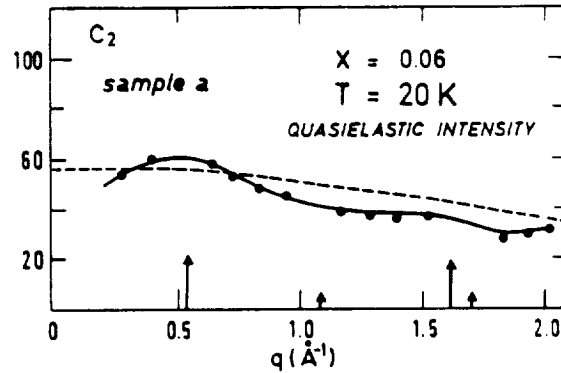
$$S(q,\omega) = c_2 \frac{\hbar\omega/kT}{e^{\hbar\omega/kT} - 1} \times \frac{\Gamma}{\Gamma^2 + (\hbar\omega)^2} \times \frac{1}{\pi} \quad (1)$$

where c_2 and Γ are respectively the norm and the width of the quasielastic signal. c_2 is equal to $kT f^2(q) \chi(q)$ where $f(q)$ is the magnetic form factor of iron and $\chi(q)$ the static susceptibility. The fits were performed in an energy range $(-1.5, 2)$ meV where the phonon contribution was small and could be adjusted at each temperature as an energy-independent background.

a) q-Dependence of the Intensities

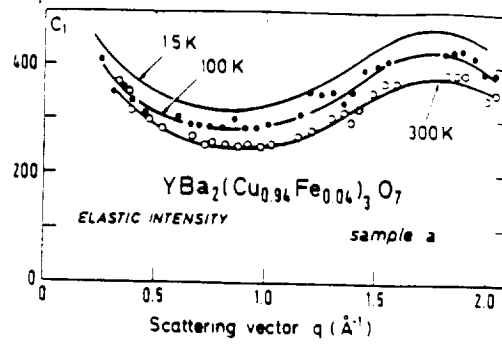
As shown in Fig. 6, the quasielastic intensity $c_2(q)$ mainly reflects the variation of $f^2(q)$ ($f(q) \simeq e^{-0.06 q^2}$ in the measured q-range), which shows that the Fe spins are almost uncorrelated. Slight enhancements around the Bragg peak positions suggest some short range ferromagnetic correlations. The quasielastic width Γ remains q-independent up to $q = 1.5 \text{ \AA}^{-1}$ and increases beyond. The q-dependence of c_2 and Γ remains the same in all the measured temperature range.

Fig.6. Quasi-elastic intensity $c_2(q)$ measured at 20 K in sample a. The dashed line is proportional to the magnetic iron form factor $f^2(q)$. The solid lines are a guide to the eye. The arrows indicate the Bragg peak positions.



The elastic intensity $c_1(q)$ is shown in Fig.7 for the sample a at several temperatures. In this very clean sample we clearly observe a large modulation of the intensity between the Bragg peaks which correspond to short range ordering effects. In order to analyse these effects quantitatively, experiments on a single crystal would be necessary. We note that this modulation is unlikely due to some ordering between the iron atoms since the rather small difference between the coherent scattering lengths of the Cu and Fe atoms induces a very low contrast. Most probably it reflects the existence of short range ordering effects between the oxygens which could be either intrinsic or induced by the iron substitution. In the other sample b, the presence of many small peaks of impurities prevents the observation of modulations of the elastic intensity.

Fig.7. Elastic intensity $c_1(q)$ measured in sample a at several temperatures. The solid lines are a guide to the eye.



b. Temperature Dependence of the Intensities

The parameters c_1 , c_2 and Γ are plotted versus temperature in Fig. 8 for the sample a. We consider successively the high temperature regime (around and above T_c), and the low temperature one (around T_f).

In the first regime, which corresponds to a paramagnetic state, the elastic intensity c_1 smoothly increases with decreasing temperature, showing no anomaly at T_c . This increase probably reflects the decrease of the Debye Waller factor, being similar to the behavior observed in $\text{YBa}_2\text{Cu}_3\text{O}_7$. The quasielastic intensity c_2 is almost temperature independent at high temperature, which shows that the susceptibility follows a Curie Law ($\chi \propto 1/T$); it increases slightly when approaching T_c from above and shows a stronger increase below T_c . This anomaly at T_c was more apparent in the intensities I_1 and I_2 obtained by integration. The quasielastic width Γ shows an intricate temperature dependence. It decreases between 300 K and 200 K then further increases and exhibits a change of slope at T_c .

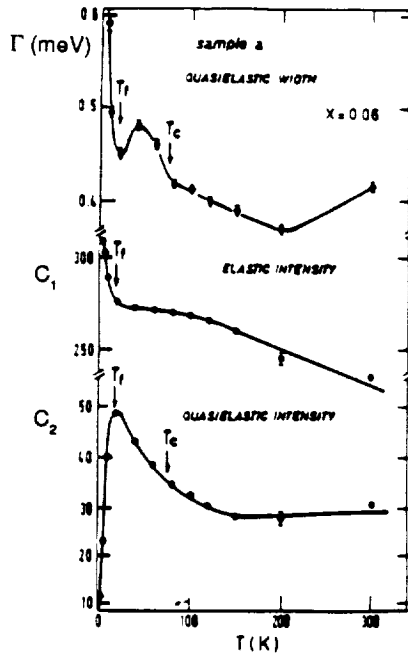


Fig.8. Elastic intensity c_1 , quasi-elastic intensity c_2 and quasi-elastic width Γ (meV) measured at $q \sim 0.7 \text{ \AA}^{-1}$ in the sample (a), versus temperature.

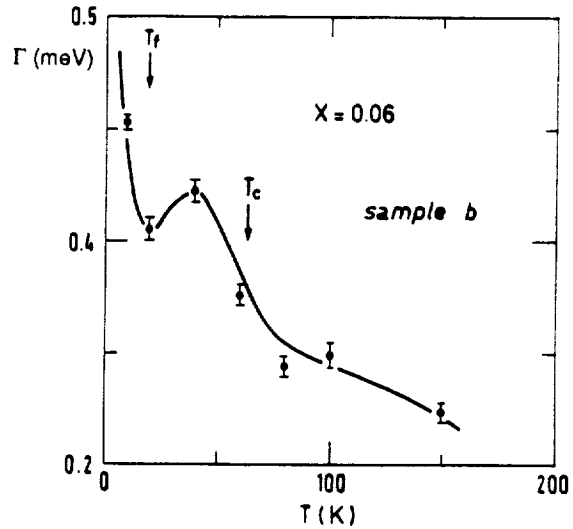


Fig.9. Quasielastic width Γ (meV) measured in sample b versus temperature.

In the low temperature regime, we observe the usual characteristics of a spin glass freezing, as previously reported in metallic spin glasses⁷ and in a $x=0.12$ sample⁴, namely a sharp increase of the elastic intensity c_1 , and a decrease of the quasielastic intensity c_2 . Moreover, we can ascertain that around T_f , the linewidth Γ exhibits a minimum, as previously suggested from measurements at $x=0.12$.⁴ The existence of this minimum was already suggested in archetypal spin glasses AuFe and CuMn⁷. It has been recently confirmed by us in another metallic spin glass α -FeMn. All the features observed at low temperature can be understood on the basis of spin clusters. The freezing of clusters of coupled spins yields a progressive transfer from the quasielastic signal to the resolution limited "elastic" one. The decrease of Γ when the temperature approaches T_f from above corresponds to an increase of the typical relaxation time within the clusters ($\Gamma \sim 1/\tau$). Its further increase is more surprising: it reveals a change in the distribution of the relaxation times which could be understood within the fractal cluster model of Malozemov and Barbara⁸ as suggested in reference 4.

The above results represent a considerable improvement of our first measurements, due to the very high statistics which could be achieved in the ILL reactor. The spin glass freezing which occurs at low temperature is now clearly ascertained. The occurrence of a spin glass state with almost uncorrelated spins does not destroy the superconductivity. The new result is that the neutron probe provides evidence for a change in the relaxation of iron spins at the superconducting transition. It appears in the quasielastic signal but not in the elastic one. This last event was first suspected from our preliminary measurements⁴ but it is clearly ruled out in these more complete and accurate data.

The most surprising result remains the temperature dependence of Γ above and around the superconducting temperature T_c . As shown in Fig.9, this interesting behavior is also observed in the second sample b which contains some impurities and has a lower T_c value. In an attempt to analyse $\Gamma(T)$, above and around T_c , we recall that in a metal, the spin relaxation time τ , ($\Gamma \sim 1/\tau$) is mainly controlled by the electron density of states at the Fermi level. In superconducting metals, for non-interacting spins one could expect that Γ would decrease linearly with T at high temperature, following a Korringa process ($\Gamma \propto T$), and would show a much stronger decrease below T_c , corresponding to the disappearance of possible relaxation processes (those involving an energy transfer smaller than the superconducting gap). Just below T_c , where the gap is small compared to the energy transfers between the spins and the electrons, one could expect a small bump in Γ , revealing the singularity of the electron density of states which diverges at the gap edge in BCS theory⁹.

Actually, as shown by NMR experiments¹⁰ mainly, the relaxation time of the Cu nuclear spins is very different from that expected in a usual superconductor. First of all, it never follows a Korringa process above T_c , which seems to characterize the so called "normal" state of these new superconductors. Secondly, the small bump of Γ expected just below T_c is observed in some NMR experiments on the oxygen and on the Cu^I sites but not on the Cu^{II} sites of $\text{YBa}_2\text{Cu}_3\text{O}_7$. However, the strong expected decrease of Γ below T_c

is observed by NMR on the Cu^{11} sites as well, and was also observed by neutrons in recent studies of excitation between crystalline field levels¹¹. In our case, the relaxation of the iron spins which substitute for the copper is very different and calls for another explanation.

References

1. K. Moorjani et al. J. Appl. Phys. 63, 4161, 1988 ;
B. Ullman et al., Physica C 153-155, 872, 1988.
2. P. Bordet et al. Solid State Comm. 66, 435, 1988 ;
G. Roth et al., Z. Phys. B 71, 43, 1988.
3. Z.Q. Diu et al. J. Mag. Mat. Mat. 69, 221, 1987 ;
P. Imbert, G. Jehanno, J. Physique 49, 7, 1988 ;
P. Dalmas de Reotier et al., Proceedings of the ICM Conf. Paris 1988, J. Phys. Coll. 1989.
T. Tamaki et al., Solid. State Comm. 65, 43, 1988.
4. I. Mirebeau et al., Europhys. Lett. 9, 181, 1989 and J. Appl. Phys. 90 ;
M. Hennion et al., Physica C 159, 124, 1989.
5. I. Mirebeau et al., Proceedings of the MMM Conference 1989, to be published in J. Appl. Phys. 1990
6. T.J. Kistenmacher, Phys. Rev. B 38, 8862, 1988 ;
Z.Q. Qiu, Y.W. Du, H. Tang, J.C. Walker, Proceedings of the MMM Conf., Boston 1989, to appear in J. Appl. Phys. 1990.
7. A.P. Murani, J. Phys. (Paris) Coll. 39, 1517, 1978 ; Proceedings of the Conference on Inelastic Neutron Scattering, Vienna vol.2, 213, 1977
8. A.P. Malozemov, B. Barbara, J. Appl. Phys. 57, 3140, 1985
9. L.C. Hebel, C.P. Slichter, Phys. Rev. 113, 1504, 1959.
10. M. Mali et al., Phys. Lett. A, 112, 1987 ;
Y. Kitaoka et al., Proceedings of the ICCF6 Conference, July, 1988, Frankfurt ;
P.C. Hammel et al., Phys. Rev. Lett. 63, 1992, 1989.
11. R. Fiele et al., Phys. Rev. Lett. 47, 610, 1981 ; U. Walker et al., Phys. Rev. B 36, 8899, 1987 ; Physica C 153-155, 1988